Cell Reports

Divergent Role for STAT5 in the Adaptive Responses of Natural Killer Cells

Graphical Abstract

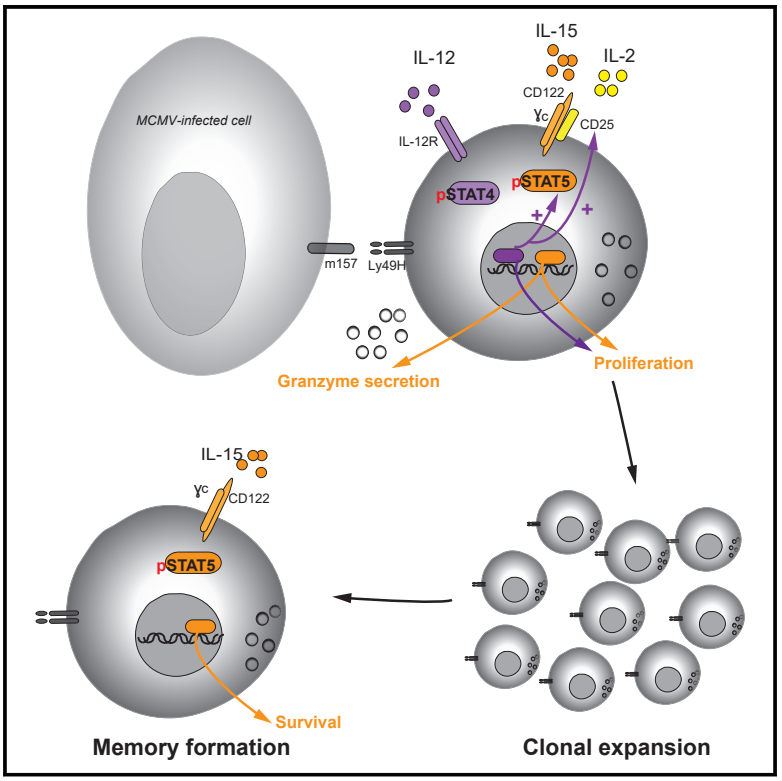

Highlights

- STAT5 is induced in NK cells by IL-12 via STAT4 during MCMV infection
- NK cells require STAT5 for protection against viral infection
- IL-2 and IL-15 non-redundantly drive clonal proliferation of anti-viral NK cells
- IL-15 and STAT5 promote NK cell survival during the memory phase

Authors

Gabriela M. Wiedemann, Simon Grassmann, Colleen M. Lau, ..., Georg Gasteiger, John J. O'Shea, Joseph C. Sun

Correspondence

sunj@mskcc.org

In Brief

Wiedemann et al. demonstrate that *Stat5a* and *Stat5b* are induced by IL-12 and STAT4 signaling in NK cells following MCMV infection. They further provide evidence that the cytokines IL-2 and IL-15 upstream of STAT5 differentially promote the early and late stages of the adaptive NK cell response to MCMV infection.

Wiedemann et al., 2020, Cell Reports *33*, 108498
December 15, 2020
https://doi.org/10.1016/j.celrep.2020.108498

CellPress

Cell Reports

CellPress
OPEN ACCESS

Report

Divergent Role for STAT5 in the Adaptive Responses of Natural Killer Cells

Gabriela M. Wiedemann,[1,2] Simon Grassmann,[1] Colleen M. Lau,[1] Moritz Rapp,[1] Alejandro V. Villarino,[3] Christin Friedrich,[4] Georg Gasteiger,[4] John J. O'Shea,[3] and Joseph C. Sun[1,5,6,*]

[1]Immunology Program, Memorial Sloan Kettering Cancer Center, New York, NY 10065, USA
[2]Department of Internal Medicine II, Technical University of Munich, Munich, Germany
[3]Molecular Immunology and Inflammation Branch, National Institute of Arthritis and Musculoskeletal and Skin Diseases, National Institutes of Health, Bethesda, MD, USA
[4]Würzburg Institute of Systems Immunology, Julius-Maximilians-Universität, 97078 Würzburg, Germany
[5]Department of Immunology and Microbial Pathogenesis, Weill Cornell Medical College, New York, NY 10065, USA
[6]Lead Contact
*Correspondence: sunj@mskcc.org
https://doi.org/10.1016/j.celrep.2020.108498

SUMMARY

Natural killer (NK) cells are innate lymphocytes with the capacity to elicit adaptive features, including clonal expansion and immunological memory. Because signal transducer and activator of transcription 5 (STAT5) is essential for NK cell development, the roles of this transcription factor and its upstream cytokines interleukin-2 (IL-2) and IL-15 during infection have not been carefully investigated. In this study, we investigate how STAT5 regulates transcription during viral infection. We demonstrate that STAT5 is induced in NK cells by IL-12 and STAT4 early after infection and that partial STAT5 deficiency results in a defective capacity of NK cells to generate long-lived memory cells. Furthermore, we find a functional dichotomy of IL-2 and IL-15 signaling outputs during viral infection, whereby both cytokines drive clonal expansion, but only IL-15 is required for memory NK cell survival. We thus highlight a role for STAT5 signaling in promoting an optimal anti-viral NK cell response.

INTRODUCTION

Natural killer (NK) cells, traditionally classified as lymphoid cells of the innate immune system, have in recent years been demonstrated to elicit a number of adaptive immune features (Rapp et al., 2018). In response to mouse cytomegalovirus (MCMV) infection, NK cells expressing the activating surface receptor Ly49H have the capacity to recognize the virally encoded glycoprotein m157 on MCMV-infected cells. This recognition leads to activation and robust clonal expansion, followed by contraction of effector NK cells, and ultimately results in the formation of a pool of long-lived memory NK cells capable of undergoing a rapid, antigen-specific recall response (Sun et al., 2009a). In addition to antigen receptor signaling, this process is driven by a complex interplay of a range of pro-inflammatory cytokines and downstream transcription factors, resulting in epigenetic and transcriptional changes within the NK cells (Lau et al., 2018).

Signal transducer and activator of transcription (STAT) factors are key regulators of NK cell functions. STAT1 and STAT2 (downstream of type 1 interferon [IFN] signaling) and STAT4 (downstream of interleukin-12 [IL-12] signaling) promote adaptive NK cell responses to MCMV in a non-redundant manner, with deficiency in one of these factors resulting in defective NK cell expansion and memory formation (Rapp et al., 2018). STAT5 is the downstream transcription factor shared by all common gamma chain (γ_c) cytokines and is required for NK cell development, maturation, survival, and cytotoxicity (Eckelhart et al., 2011; Friedmann et al., 1996; Gotthardt and Sexl, 2016; Imada et al., 1998; Johnston et al., 1995). NK-cell-intrinsic STAT5 deficiency results in severely reduced NK cell numbers and NK-cell-mediated tumor control in mice (Gotthardt et al., 2016; Imada et al., 1998; Villarino et al., 2017). Because of the detrimental impact of STAT5 deficiency on NK cells, functional studies on STAT5-deficient NK cells are limited, and the role of STAT5 during anti-viral NK cell responses remains to be investigated.

The two most functionally relevant γ_c cytokines for NK cells are thought to be IL-2 and IL-15. Both cytokines signal through the γ_c and the shared intermediate affinity heterodimeric receptor consisting of the IL-2 receptor (IL-2R) β chain (CD122), although each cytokine preferentially binds to this receptor complex in the presence of its own distinct high-affinity α chain (IL-2Rα [CD25] and IL-15Rα) (Sugamura et al., 1996). CD25 is expressed together with the γ_c and CD122 to form the high-affinity IL-2R on the NK cell surface upon activation, whereas IL-15Rα is expressed by neighboring cells, including dendritic cells and macrophages, and predominantly *trans*-presents IL-15 to cells that express the γ_c and CD122 chains (Leonard et al., 2019). Despite their shared receptor subunits and downstream signaling pathways,

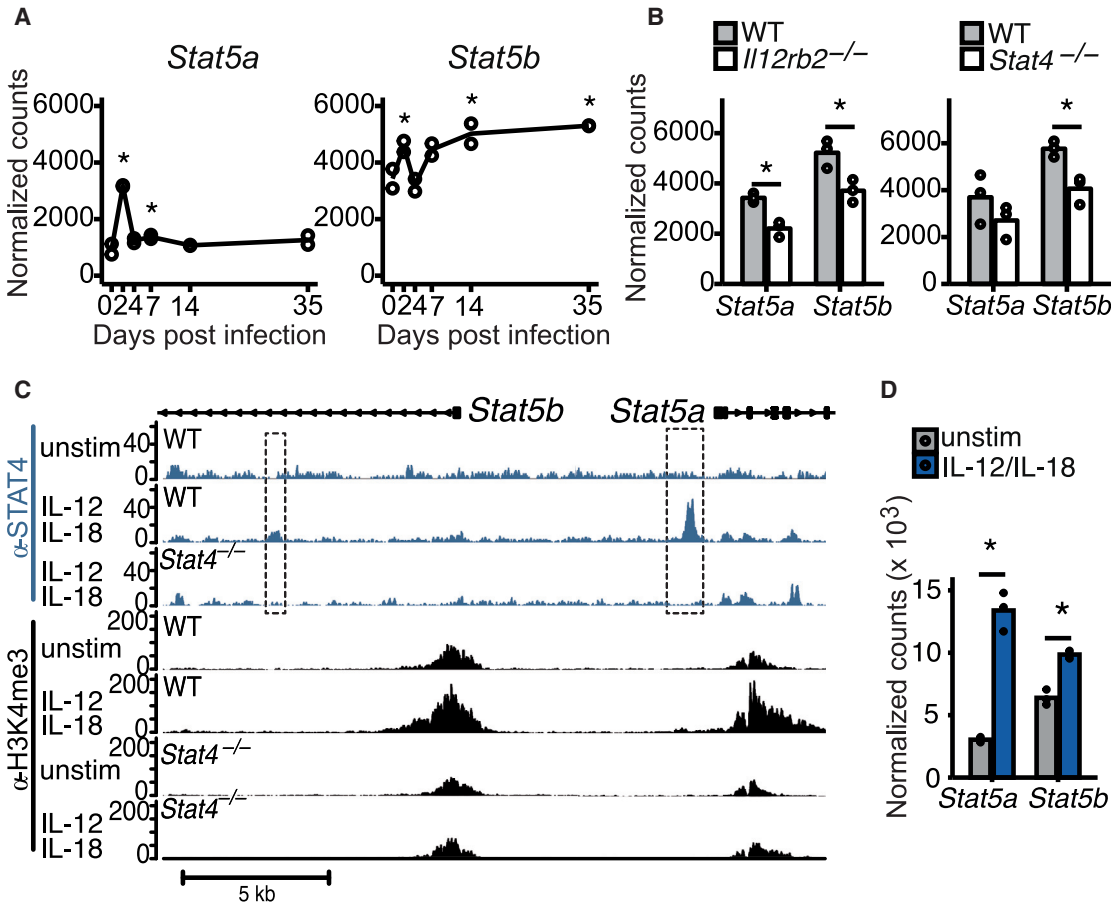

Figure 1. IL-12- and STAT4-Dependent Induction of STAT5 in NK Cells during MCMV Infection

(A) RNA-seq was performed on Ly49H$^+$ NK cells on days 0, 2, 4. 7, 14, and 35 of MCMV infection. Normalized counts of *Stat5a* and *Stat5b* are displayed.

(B) RNA-seq on WT versus *Il12rb2*$^{-/-}$ or *Stat4*$^{-/-}$ from mixed BMC mice on day 2 PI. Normalized counts of *Stat5a* and *Stat5b* are displayed.

(C) ChIP-seq was performed for STAT4 and H3K4me3 on WT and *Stat4*$^{-/-}$ NK cells cultured in media alone (unstim) or with IL-12 and IL-18. Representative gene tracks of mapped STAT4 ChIP (blue tracks) or H3K4me3 ChIP (black tracks) are displayed.

(D) NK cells were cultured in media (unstim) or with IL-12 + IL-18, and RNA-seq was performed after 3 h of culture. Normalized counts of *Stat5a* and *Stat5b* are displayed.

Error bars indicate SEM.

IL-2 and IL-15 are thought to elicit distinct functions in NK cells. IL-15 is required for NK cell development and survival (Kennedy et al., 2000; Koka et al., 2003), whereas deficiency in IL-2 signaling does not affect NK cell numbers but impairs NK cell activation and target cell killing (Gasteiger et al., 2013; Kündig et al., 1993). During infection, T-cell-derived IL-2 has been implicated in aiding NK cell responses in a mouse model of Leishmania infection (Bihl et al., 2010), and early upregulation of the high-affinity IL-2R during MCMV infection suggests a functional requirement in the early response (Lee et al., 2012). However, despite decades of culturing mouse and human NK cells using IL-2, an *in vivo* role for this cytokine in NK cell responses has not been stringently investigated using models of genetic ablation. Here, we provide a detailed analysis of the role of STAT5 and upstream IL-2 versus IL-15 signaling in the early and adaptive phases of NK cell response to viral infection and describe divergent transcriptional changes driven by these distinct signaling pathways.

RESULTS AND DISCUSSION

STAT5 Is Transcriptionally and Epigenetically Regulated by IL-12 and STAT4 Early after MCMV Infection

We first investigated mRNA levels of STAT5 in NK cells throughout the course of MCMV infection. STAT5 is encoded by two adjacent genes in mammals, namely, *Stat5a* and *Stat5b*, of which *Stat5b* has a greater impact on NK cells (Imada et al., 1998; Villarino et al., 2017). During the course of infection, we found that both *Stat5a* and *Stat5b* mRNA peaked on day 2 post-infection (PI) (Figure 1A), with transcript levels returning to initial levels by day 4 PI. Interestingly, *Stat5b* mRNA then increased at later time points and was found at significantly higher levels in memory NK cells than in naive NK cells (Figure 1A), suggesting a functional requirement for STAT5 in both early and late NK cell responses against MCMV infection.

To determine whether exposure to pro-inflammatory cytokines led to the induction of *Stat5* in NK cells after MCMV infection, we performed RNA sequencing (RNA-seq) on NK cells isolated from wild-type (WT), IL-12-receptor-deficient (*Il12rb2*$^{-/-}$), or STAT4-deficient (*Stat4*$^{-/-}$) mice at day 2 PI. Interestingly, *Stat5* induction was significantly reduced in NK cells lacking IL-12R or STAT4 on day 2 PI (Kaplan et al., 1996; Wu et al., 2000; Figure 1B), whereas IL-12 receptor deficiency did not affect *Stat5* levels in uninfected NK cells (Figure S1A). No decreases in *Stat5* were observed in NK cells lacking interferon α/β receptor (IFNAR) or STAT1, with the *Stat5a* transcript even increased in *Stat1*$^{-/-}$ NK cells (Meraz et al., 1996; Figure S1B), suggesting that IL-12 signaling by STAT4 is the main inducer of STAT5 and that STAT1 inhibits *Stat5a* induction. To further support our hypothesis, we observed STAT4 binding at the *Stat5a* promoter and at a *Stat5b* intronic region by chromatin immunoprecipitation sequencing (ChIP-seq) in WT but not STAT4-deficient NK cells stimulated with IL-12 and IL-18 (Figure 1C). We also found an increased deposition of the permissive histone mark H3K4me3 at the *Stat5a* and *Stat5b* promoter regions of NK cells during IL-12 and IL-18 stimulation, which was abrogated in *Stat4*$^{-/-}$ NK cells receiving the same stimuli (Figure 1C). Moreover, stimulation with IL-12 and IL-18 also led to a significant upregulation of *Stat5a* and *Stat5b* transcripts in NK cells (Figure 1D). Altogether, these data suggest that IL-12 signaling in NK cells causes STAT4 to directly target the *Stat5* loci, thus influencing the epigenetic landscape and enabling increased transcription of *Stat5* in response to viral infection.

STAT5 Is Required for Optimal NK Cell Responses to MCMV Infection

To investigate a functional role for STAT5 in NK cells during MCMV infection, we generated mice with an NK-cell-selective deletion of *Stat5a* and *Stat5b* (*NK*^{Cre} × *Stat5*$^{fl/fl}$). When we infected *Stat5*$^{fl/fl}$, *NK*^{Cre} × *Stat5*$^{fl/+}$, and *NK*^{Cre} × *Stat5*$^{fl/fl}$ mice with MCMV, we observed that *NK*^{Cre} *x Stat5f*$^{l/fl}$mice containing Stat5-deficient NK cells showed significantly greater mortality and viral load (Figure 2A). Furthermore, using *NK*^{Cre} × *Stat5*$^{fl/+}$: WT mixed bone marrow chimeric (mBMC; Figure S2A) mice (because *NK*^{Cre} × *Stat5*$^{fl/fl}$ lack NK cells [Eckelhart et al., 2011] and mBMC mice allow for investigation of WT and STAT5-deficient NK cells in the same environment), we observed that even NK cells with heterozygous STAT5 levels had reduced granzyme A and B production at day 2 PI (Figure 2B) and were less mature both at steady state and on day 2 PI (Figures 2C, S2B, and S2C). Thus, we conclude that STAT5 in NK cells is required for proper NK cell maturation under steady-state conditions and for optimal NK cell effector functions during MCMV infection.

To determine the direct downstream targets of STAT5 during MCMV infection, we performed RNA-seq on WT and *NK*^{Cre} × *Stat5*$^{fl/+}$ NK cells from mBMC mice on day 2 PI and overlapped the genes differentially expressed (DE) with STAT5 target genes defined by ChIP-seq. Interestingly, only a small number of genes DE in *NK*^{Cre} × *Stat5*$^{fl/+}$ NK cells was found to be STAT5 bound (38 out of 503 DE genes in total) (Figure 2D). The high percentage of DE non-STAT5 target genes might be attributable to a compensatory activation of other pathways, such as the tumor necrosis factor receptor superfamily pathways (TNFRSFs) (Villarino et al., 2017). Among the STAT5 target genes DE at day 2 PI, the number of genes upregulated and downregulated were similar (Figure 2D). Importantly, STAT5-bound genes with significantly lower expression in *NK*^{Cre} × *Stat5*$^{fl/+}$ NK cells on day 2 PI included *Gzma*, *Gzmb*, *Klrg1*, and Ly49 genes (*Klra1* and *Klra9*), whereas RNA-seq of uninfected NK cells revealed no changes in granzyme levels in STAT5-deficient NK cells (Figures 2E, 2F, and S2C). These findings underscore the requirement of STAT5 for proper NK cell maturation and cytotoxicity during infection.

Finally, we tested whether STAT5 was required for the adaptive features of anti-viral NK cells. Using an adoptive transfer model in which WT and *NK*^{Cre} × *Stat5*$^{fl/+}$ NK cells were derived from mBMC mice (Figure S2D), we observed that NK cells with heterozygous STAT5 levels had a pronounced defect in clonal expansion compared with WT NK cells following MCMV infection (Figures 2G and S2D), resulting in a reduced pool of memory NK cells in liver and spleen at 4 weeks PI (Figure 2H). Moreover, *NK*^{Cre} × *Stat5*$^{fl/+}$ memory NK cells showed a diminished expression of the maturation marker KLRG1 compared to WT controls (Figure 2H). Altogether, these findings suggest that STAT5 in NK cells mediates a multitude of critical effector functions that underlie protective host responses against viral infection.

Non-redundant Requirement for IL-2 and IL-15 during NK Cell Clonal Expansion

In order to elucidate the importance and contribution of specific signaling pathways upstream of STAT5, we used mice with NK cells containing a tamoxifen-inducible deficiency in the shared IL-2/IL-15Rβ chain CD122 (*Ubc*$^{Cre\text{-}ERT\text{-}2}$ × *Il2rb*$^{fl/fl}$) or high-affinity IL-2Rα chain CD25 (*NK*^{Cre} × *Cd25*$^{fl/fl}$). Reduced expression of CD122 and CD25 on NK cells was confirmed by flow cytometry (Figures S3A and S3B). In adoptive co-transfer experiments of WT and CD25- or CD122-deficient NK cells, both CD25-deficient and CD122-deficient NK cells were significantly outcompeted by WT NK cells during the first week after MCMV infection and continued to show diminished numbers at memory time points (Figure 3A). To understand how these signaling pathways drive NK cell expansion during MCMV exposure, we measured the proliferation of adoptively transferred WT or knockout (KO) NK cells labeled with cell tracer violet (CTV) (Figure S3E). Both CD25- and CD122-deficient NK cells displayed reduced proliferation compared to WT NK cells as early as day 3 PI (Figure 3B), indicating a requirement of IL-2 and possibly IL-15 during clonal expansion.

In order to further delineate the requirement of IL-2 versus IL-15 in promoting NK cell expansion, we neutralized either IL-2 or IL-15 by using antibodies from day −1 to 4 PI in mice adoptively transferred with WT NK cells and infected with MCMV (Figure S3F). Interestingly, neutralization of either cytokine resulted in decreased NK cell proliferation, measured by Ki67 expression on day 4 PI (Figure 3C). Similarly, blockade of either IL-2 or IL-15 resulted in decreased granzyme A production (Figure 3D), highlighting a non-redundant role for both cytokines in driving NK cell expansion and cytotoxicity during MCMV infection.

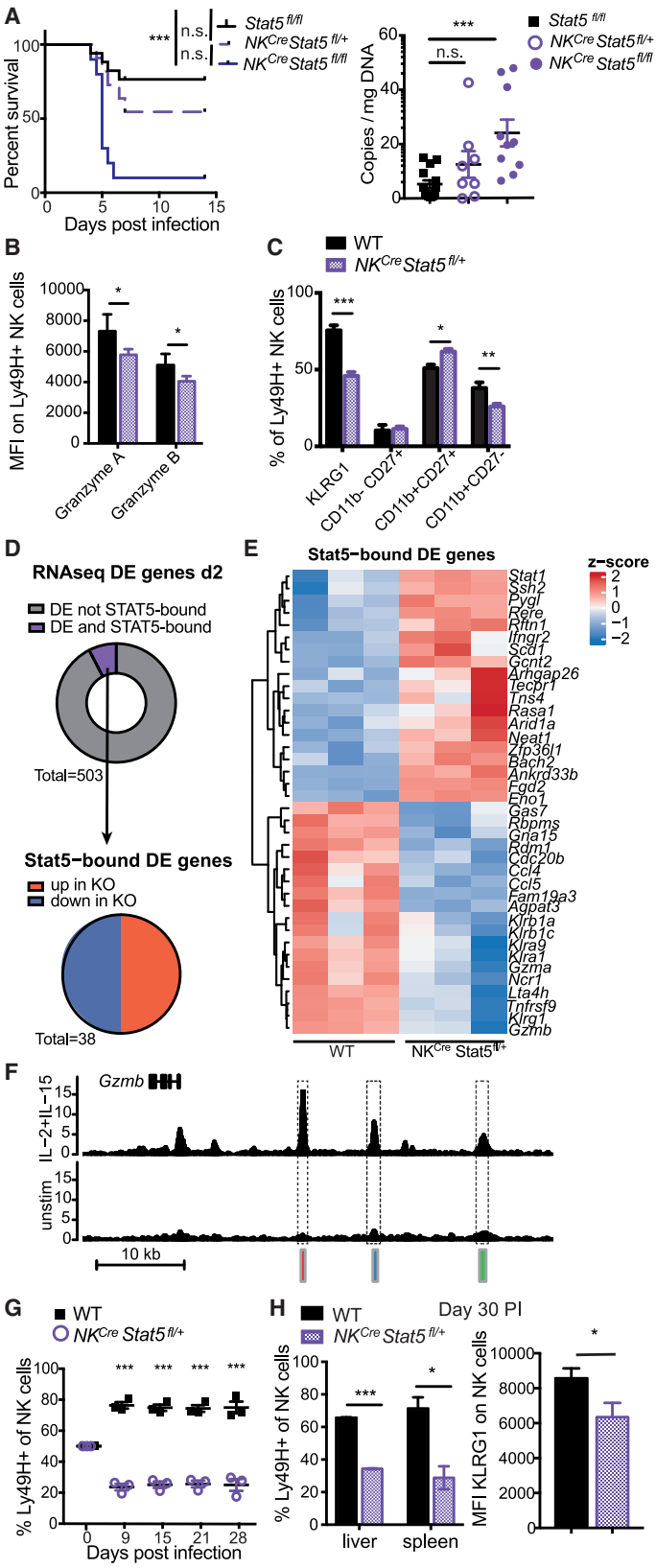

Figure 2. STAT5-Dependent Anti-viral NK Cell Response

(A) *Stat5*$^{fl/fl}$, *NK*^{Cre} × *Stat5*$^{fl/+}$, and *NK*^{Cre} × *Stat5*$^{fl/fl}$ mice were infected with high-dose MCMV. Viral titers in the serum were measured on day 4 PI. Data are representative of 2 independent experiments (n = 4–6).

(B and C) Mixed WT:*NK*^{Cre} *x Stat5*$^{fl/+}$ BMC mice were infected with MCMV. Ly49H^{+} WT or *NK*^{Cre} × *Stat5*$^{fl/+}$ NK cells from spleen were analyzed on day 2 PI for granzyme A and B expression (B) or indicated activation/maturation markers (C). Data are representative of at least 2 independent experiments (n = 4).

(D) RNA-seq was performed on Ly49H^{+} WT or *NK*^{Cre} × *Stat5*$^{fl/+}$ NK cells at day 2 PI (n = 3). ChIP-seq was performed on NK cells stimulated with IL-2 and IL-15 for 3 h. Donut graph displays the proportion of DE genes (adjusted p value [p_{adj}] < 0.05) that are STAT5 bound (purple). Pie graph displays STAT5-bound DE genes (p_{adj} < 0.05) categorized by direction of gene expression.

(E) Heatmap shows *Z* scores of all DE and STAT5-bound genes described in (D).

(F) Representative gene tracks of mapped STAT5 ChIP.

(G and H) Splenocytes from mixed WT:*NK*^{Cre} × *Stat5*$^{fl/+}$ BMC mice were adoptively transferred into *Rag2*$^{-/-}$ × *Ly49h*$^{-/-}$ mice and infected with MCMV. (G) Graph shows the relative WT to *NK*^{Cre} × *Stat5*$^{fl/+}$ NK cell percentages that were measured over the course of infection. (H) Bar graphs show percentage of memory Ly49H^{+} WT and *NK*^{Cre} × *Stat5*$^{fl/+}$ NK cells in spleen and liver and KLRG1 surface expression (liver) on day 30 PI. Data are representative of 2 independent experiments (n = 3–4).

All error bars indicate SEM.

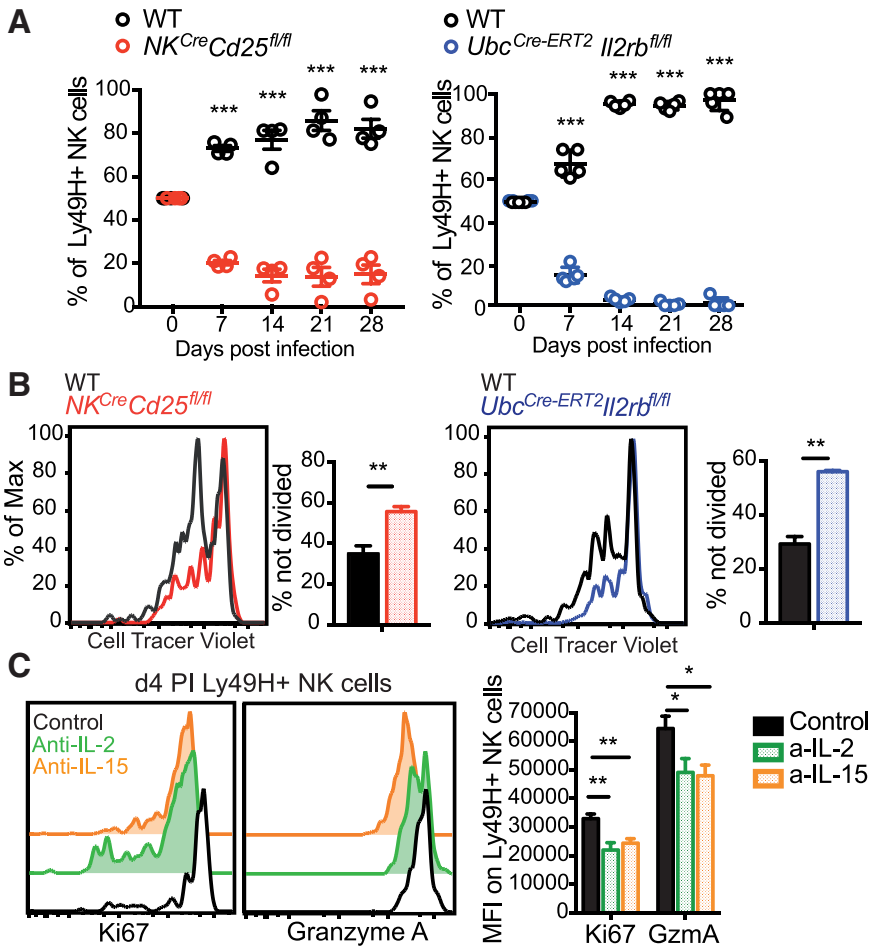

Figure 3. Both IL-2 and IL-15 Drive NK Cell Expansion *In Vivo*

(A) Equal numbers of WT and $Ubc^{Cre\text{-}ERT2}$ × $Il2rb^{fl/fl}$ or NK^{Cre} × $CD25^{fl/fl}$ NK cells were transferred into $Ly49h^{-/-}$ mice, followed by infection with MCMV. Donor $Ubc^{Cre\text{-}ERT2}$ × $Il2rb^{fl/fl}$ mice were treated with tamoxifen on days −3, −2, and −1 prior to adoptive transfer. Following MCMV infection, relative percentages of $Ly49H^+$ WT and KO NK cells are displayed (n = 4–5).

(B) NK cells from WT mice, NK^{Cre} × $CD25^{fl/fl}$ mice, or $Ubc^{Cre\text{-}ERT2}$ × $Il2rb^{fl/fl}$ mice treated with tamoxifen on days −3, −2, and −1 were labeled with CTV and transferred into $Ly49h^{-/-}$ mice, followed by infection with MCMV. Representative flow plots and graphs show amounts of undivided WT and KO NK cells from the liver at day 3 PI.

(C) WT $Ly49H^+$ NK cells were transferred into $Ly49h^{-/-}$ mice treated followed by infection with MCMV and treatment with PBS, anti-IL-2, or anti-IL-15 on days -1 to 4 PI. Flow plots and graph show amount of Ki67 and granzyme A on transferred $Ly49H^+$ NK cells at day 4 PI. Data are pooled from 2 independent experiments (n = 4–5). All error bars indicate SEM.

Memory NK Cell Survival during the Contraction Phase Is STAT5 Dependent

Finally, we investigated how STAT5 and IL-2 versus IL-15 shape the contraction and memory phases of the NK cell response. To this end, we generated $Ubc^{Cre\text{-}ERT2}$ × $Stat5^{fl/fl}$ mice that allow for inducible deletion of STAT5 in NK cells upon tamoxifen treatment. Following adoptive transfer of WT and $Ubc^{Cre\text{-}ERT2}$ × $Stat5^{fl/fl}$ NK cells and infection with MCMV, recipient mice were treated with tamoxifen or oil at days 8 to 10 PI, immediately following the peak of the clonal expansion of NK cells (Figure 4A). Within a week after tamoxifen treatment, STAT5-deleted NK cells were outcompeted by WT NK cells, resulting in a reduced memory NK cell pool in tamoxifen-treated mice (Figure 4B). We determined the level of activated caspases by fluorochrome inhibitor of caspases (FLICA) staining (as a measure of apoptosis) in NK cells on day 13 PI and found increased FLICA incorporation in STAT5-deleted NK cells (Figure 4C). In order to discriminate between the function of IL-2 versus IL-15 during the maintenance of memory NK cells, we treated mice with antibodies against IL-2 or IL-15 between days 8 and 18 PI (Figure S3). In contrast to our findings during the expansion phase, only IL-15 neutralization resulted in diminished numbers of memory NK cells (Figure 4D), suggesting a differential role for these γ_c cytokines during the distinct phases of the NK cell response against viral infection.

In summary, our data suggest that STAT5 is required throughout the course of MCMV infection for optimal NK cell responses. During the expansion phase, STAT5 drives NK cell maturation and cytotoxicity, and STAT5 deficiency in NK cells resulted in an increased susceptibility to MCMV. Our data suggest that STAT5 is induced by IL-12 through direct STAT4 binding at the *Stat5* loci early after MCMV infection, which is a mechanism similar to the IL-12-mediated and STAT4-dependent induction of its upstream receptor CD25 (Lee et al., 2012). Interestingly, STAT5 and CD25 expression peak at nearly the same time following infection (~day 2 PI), and here, we demonstrate a functional impact for IL-2 signaling during the early anti-viral NK cell response. This apparent cooperative interaction between STAT4 and STAT5 transcription factors represents the mechanistic opposite of the previously reported cross-regulatory antagonism that occurs with STAT4 and STAT1 (Lau et al., 2018). Interestingly, because the *Stat5a* transcript was upregulated in $Stat1^{-/-}$ NK cells early after infection, we may be observing an antagonism between STAT4 and STAT1 in the regulation of *Stat5*, as has been previously described for the induction of IFN-γ (Nguyen et al., 2000).

During the proliferative burst of NK cells in response to MCMV infection, both IL-2 and IL-15 and their respective receptors CD25 and CD122 are required in a non-redundant manner. Although IL-2 has been used for decades to grow NK cells *in vitro*, and a putative role for IL-2 during NK cell proliferation had been suggested (Lee et al., 2012; Nandagopal et al., 2014), it was previously reported that IL-15- and γ_c-independent

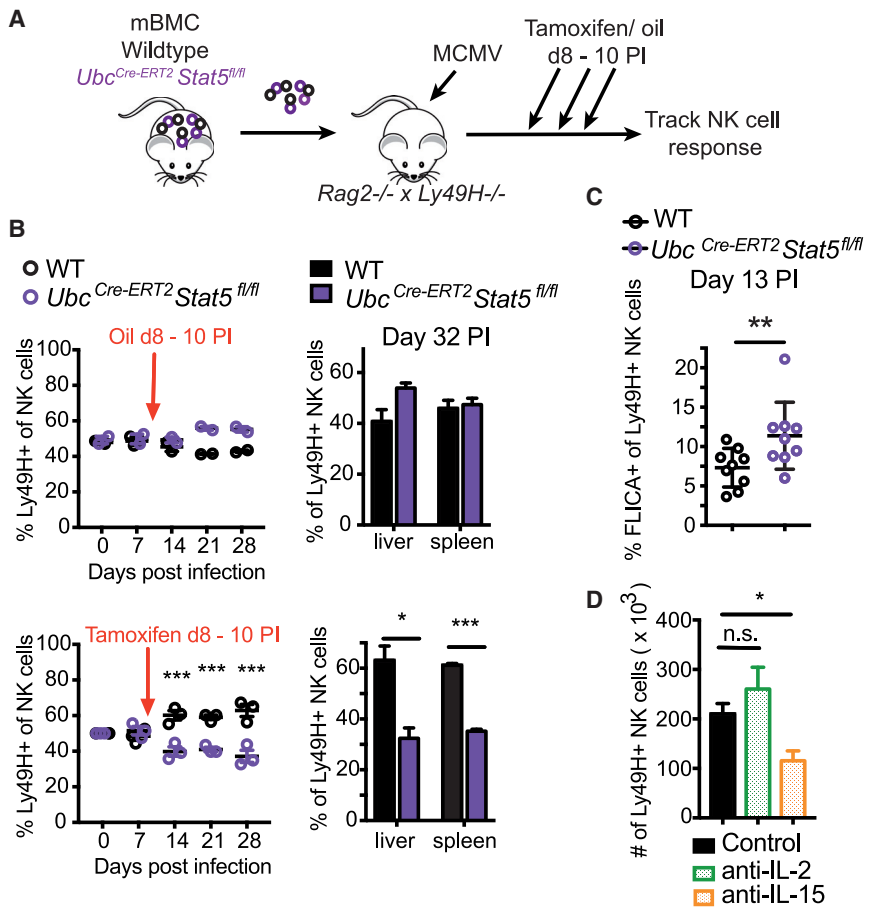

Figure 4. IL-15 and STAT5 Are Required for the Survival of Memory NK Cells

(A–C) Splenic NK cells from WT:*Ubc*$^{Cre\text{-}ERT2}$ × *Stat5*$^{fl/fl}$ mBMC mice were transferred into *Rag2*$^{-/-}$ × *Ly49h*$^{-/-}$ mice. Tamoxifen or oil (as a control) was administered on days 8 to 10 following MCMV infection. (B) Graphs show relative percentages of Ly49H^{+} WT and KO NK cells in the peripheral blood at indicated time points and in spleen and liver at day 32 PI. Data are representative of 2 independent experiments (n = 2–4). (C) Graph shows percentage of NK cells from spleen staining positive for FLICA on day 13 PI. Data are pooled from 2 independent experiments (n = 4–5).

(D) WT Ly49H^{+} NK cells were transferred into *Ly49h*$^{-/-}$ mice infected with MCMV, and recipient mice were treated with PBS, anti-IL-2, or anti-IL-15 from days 8 to 18 PI. Graph shows the number of NK cells in the spleen on day 30 PI. Data are representative of 2 independent experiments (n = 4–5).

All error bars indicate SEM.

NK cell expansion could occur during MCMV infection (Sun et al., 2009b). However, in a competitive setting *in vivo*, we now observe a reduced capacity of NK cells deficient in STAT5, CD25, or CD122 to generate a robust anti-viral response or long-lived memory pool. Although IL-12 may be sufficient to drive some expansion in the absence of γ_c signaling (Sun et al., 2009b), optimal NK cell responses require non-redundant IL-2 and IL-15 signaling. In contrast to the expansion phase, IL-15 signaling by STAT5 is sufficient to sustain memory NK cell survival during the contraction phase in the absence of IL-2 signaling. Because IL-2 and IL-15 use the same receptor β and γ chain and the intracellular signaling cascade driven by either cytokine is very similar (Ring et al., 2012), the observed differences in memory NK cell generation may be due to both a lack of CD25 expression on NK cells during the late stages of infection and lower local and systemic IL-2 levels (data not shown). Our findings thus reveal a functional dichotomy between IL-2 and IL-15 in anti-viral NK cells—one that is shared by CD8^{+} T cells (Becker et al., 2002; Mitchell et al., 2010; Schluns et al., 2002), whereby IL-2 predominantly drives proliferation and effector differentiation, but IL-15 alone promotes survival during the contraction to memory transition.

Because the phosphatidylinositol 3-kinase (PI3K)-mammalian target of rapamycin (mTOR) signaling pathway is another major pathway downstream of IL-2 and IL-15 receptors (Ring et al., 2012) and has been implicated in both MCMV-induced NK cell expansion and mitophagy during the contraction phase (Nandagopal et al., 2014; O'Sullivan et al., 2015), we cannot exclude that abrogation of this pathway (in our receptor ablation or cytokine neutralization studies) may contribute to our findings. Nonetheless, we clearly demonstrate that STAT5 signaling is required for the formation of effector and memory NK cells during all stages of MCMV infection. Overall, our study highlights the distinct effects of two closely related cytokines and their major downstream transcription factor on NK cell functions during MCMV infection and uncovers another aspect of the complex cytokine signaling network that facilitates the anti-viral NK cell response.

STAR★METHODS

Detailed methods are provided in the online version of this paper and include the following:

- KEY RESOURCES TABLE
- RESOURCE AVAILABILITY
  - Lead contact
  - Materials availability
  - Data and code availability
- EXPERIMENTAL MODEL AND SUBJECT DETAILS
  - Mice
- METHOD DETAILS
  - Virus infection
  - Adoptive transfer studies
  - Tamoxifen and antibody treatment

- Flow cytometry and cell sorting
- ChIP-seq and analysis
- RNA-seq and analysis

- QUANTIFICATION AND STATISTICAL ANALYSIS
  - Statistical analyses

SUPPLEMENTAL INFORMATION

Supplemental Information can be found online at https://doi.org/10.1016/j.celrep.2020.108498.

ACKNOWLEDGMENTS

G.M.W. was supported by a DFG (Deutsche Forschungsgemeinschaft) research fellowship (WI4927/1-1 and WI4927/2-1). C.M.L. was supported by the Cancer Research Institute as a Cancer Research Institute-Carson Family Fellow. M.R. was supported by a fellowship from the German Academic Exchange Service (DAAD). G.G. was supported by the DFG priority programme ILCs (GA2129/2-1), the DFG Emmy Noether programme (GA2129/2-1), and the European Research Council (ERCStG 759176). J.C.S. was supported by the Ludwig Center for Cancer Immunotherapy, the American Cancer Society, the Burroughs Wellcome Fund, and the NIH (AI100874, AI130043, and P30CA008748).

AUTHOR CONTRIBUTIONS

G.M.W., C.M.L., and J.C.S. designed the study; G.M.W., S.G., M.R., and C.M.L. performed the experiments and analyzed the data; A.V.V., C.F., G.G., and J.J.O. provided critical resources; and G.M.W., C.M.L., and J.C.S. wrote the manuscript.

DECLARATION OF INTERESTS

The authors declare no competing interests.

Received: January 6, 2020
Revised: October 9, 2020
Accepted: November 17, 2020
Published: December 15, 2020

REFERENCES

Adams, N.M., Geary, C.D., Santosa, E.K., Lumaquin, D., Le Luduec, J.-B., Sottile, R., van der Ploeg, K., Hsu, J., Whitlock, B.M., Jackson, B.T., et al. (2019). Cytomegalovirus Infection Drives Avidity Selection of Natural Killer Cells. Immunity *50*, 1381–1390.e5.

Becker, T.C., Wherry, E.J., Boone, D., Murali-Krishna, K., Antia, R., Ma, A., and Ahmed, R. (2002). Interleukin 15 is required for proliferative renewal of virus-specific memory CD8 T cells. J. Exp. Med. *195*, 1541–1548.

Bihl, F., Pecheur, J., Bréart, B., Poupon, G., Cazareth, J., Julia, V., Glaichenhaus, N., and Braud, V.M. (2010). Primed antigen-specific CD4+ T cells are required for NK cell activation in vivo upon Leishmania major infection. J. Immunol. *185*, 2174–2181.

Bolger, A.M., Lohse, M., and Usadel, B. (2014). Trimmomatic: a flexible trimmer for Illumina sequence data. Bioinformatics *30*, 2114–2120.

Chinen, T., Kannan, A.K., Levine, A.G., Fan, X., Klein, U., Zheng, Y., Gasteiger, G., Feng, Y., Fontenot, J.D., and Rudensky, A.Y. (2016). An essential role for the IL-2 receptor in T_{reg} cell function. Nat. Immunol. *17*, 1322–1333.

Cui, Y., Riedlinger, G., Miyoshi, K., Tang, W., Li, C., Deng, C.X., Robinson, G.W., and Hennighausen, L. (2004). Inactivation of Stat5 in mouse mammary epithelium during pregnancy reveals distinct functions in cell proliferation, survival, and differentiation. Mol. Cell. Biol. *24*, 8037–8047.

Eckelhart, E., Warsch, W., Zebedin, E., Simma, O., Stoiber, D., Kolbe, T., Rülicke, T., Mueller, M., Casanova, E., and Sexl, V. (2011). A novel Ncr1-Cre mouse reveals the essential role of STAT5 for NK-cell survival and development. Blood *117*, 1565–1573.

Fodil-Cornu, N., Lee, S.-H., Belanger, S., Makrigiannis, A.P., Biron, C.A., Buller, R.M., and Vidal, S.M. (2008). Ly49h-deficient C57BL/6 mice: a new mouse cytomegalovirus-susceptible model remains resistant to unrelated pathogens controlled by the NK gene complex. J. Immunol. *181*, 6394–6405.

Friedmann, M.C., Migone, T.S., Russell, S.M., and Leonard, W.J. (1996). Different interleukin 2 receptor beta-chain tyrosines couple to at least two signaling pathways and synergistically mediate interleukin 2-induced proliferation. Proc. Natl. Acad. Sci. USA *93*, 2077–2082.

Gasteiger, G., Hemmers, S., Firth, M.A., Le Floc'h, A., Huse, M., Sun, J.C., and Rudensky, A.Y. (2013). IL-2-dependent tuning of NK cell sensitivity for target cells is controlled by regulatory T cells. J. Exp. Med. *210*, 1167–1178.

Gotthardt, D., and Sexl, V. (2016). STATs in NK-Cells: The Good, the Bad, and the Ugly. Front. Immunol. *7*, 694.

Gotthardt, D., Putz, E.M., Grundschober, E., Prchal-Murphy, M., Straka, E., Kudweis, P., Heller, G., Bago-Horvath, Z., Witalisz-Siepracka, A., Cumaraswamy, A.A., et al. (2016). STAT5 Is a Key Regulator in NK Cells and Acts as a Molecular Switch from Tumor Surveillance to Tumor Promotion. Cancer Discov. *6*, 414–429.

Imada, K., Bloom, E.T., Nakajima, H., Horvath-Arcidiacono, J.A., Udy, G.B., Davey, H.W., and Leonard, W.J. (1998). Stat5b is essential for natural killer cell-mediated proliferation and cytolytic activity. J. Exp. Med. *188*, 2067–2074.

Johnson, L.R., Weizman, O.E., Rapp, M., Way, S.S., and Sun, J.C. (2016). Epitope-Specific Vaccination Limits Clonal Expansion of Heterologous Naive T Cells during Viral Challenge. Cell Rep. *17*, 636–644.

Johnston, J.A., Bacon, C.M., Finbloom, D.S., Rees, R.C., Kaplan, D., Shibuya, K., Ortaldo, J.R., Gupta, S., Chen, Y.Q., Giri, J.D., et al. (1995). Tyrosine phosphorylation and activation of STAT5, STAT3, and Janus kinases by interleukins 2 and 15. Proc. Natl. Acad. Sci. USA *92*, 8705–8709.

Kaplan, M.H., Sun, Y.L., Hoey, T., and Grusby, M.J. (1996). Impaired IL-12 responses and enhanced development of Th2 cells in Stat4-deficient mice. Nature *382*, 174–177.

Kennedy, M.K., Glaccum, M., Brown, S.N., Butz, E.A., Viney, J.L., Embers, M., Matsuki, N., Charrier, K., Sedger, L., Willis, C.R., et al. (2000). Reversible defects in natural killer and memory CD8 T cell lineages in interleukin 15-deficient mice. J. Exp. Med. *191*, 771–780.

Koka, R., Burkett, P.R., Chien, M., Chai, S., Chan, F., Lodolce, J.P., Boone, D.L., and Ma, A. (2003). Interleukin (IL)-15R[α]-deficient natural killer cells survive in normal but not IL-15R[α]-deficient mice. J. Exp. Med. *197*, 977–984.

Kündig, T.M., Schorle, H., Bachmann, M.F., Hengartner, H., Zinkernagel, R.M., and Horak, I. (1993). Immune responses in interleukin-2-deficient mice. Science *262*, 1059–1061.

Langmead, B., and Salzberg, S.L. (2012). Fast gapped-read alignment with Bowtie 2. Nat. Methods *9*, 357–359.

Lau, C.M., Adams, N.M., Geary, C.D., Weizman, O.-E., Rapp, M., Pritykin, Y., Leslie, C.S., and Sun, J.C. (2018). Epigenetic control of innate and adaptive immune memory. Nat. Immunol. *19*, 963–972.

Lee, S.-H., Fragoso, M.F., and Biron, C.A. (2012). Cutting edge: a novel mechanism bridging innate and adaptive immunity: IL-12 induction of CD25 to form high-affinity IL-2 receptors on NK cells. J. Immunol. *189*, 2712–2716.

Leonard, W.J., Lin, J.X., and O'Shea, J.J. (2019). The γ_c Family of Cytokines: Basic Biology to Therapeutic Ramifications. Immunity *50*, 832–850.

Li, Q.H., Brown, J.B., Huang, H.Y., and Bickel, P.J. (2011). Measuring Reproducibility of High-Throughput Experiments. Ann. Appl. Stat. *5*, 1752–1779.

Love, M.I., Huber, W., and Anders, S. (2014). Moderated estimation of fold change and dispersion for RNA-seq data with DESeq2. Genome Biol. *15*, 550.

Meraz, M.A., White, J.M., Sheehan, K.C., Bach, E.A., Rodig, S.J., Dighe, A.S., Kaplan, D.H., Riley, J.K., Greenlund, A.C., Campbell, D., et al. (1996). Targeted disruption of the Stat1 gene in mice reveals unexpected physiologic specificity in the JAK-STAT signaling pathway. Cell *84*, 431–442.

Mitchell, D.M., Ravkov, E.V., and Williams, M.A. (2010). Distinct roles for IL-2 and IL-15 in the differentiation and survival of CD8+ effector and memory T cells. J. Immunol. *184*, 6719–6730.

Nandagopal, N., Ali, A.K., Komal, A.K., and Lee, S.-H. (2014). The Critical Role of IL-15-PI3K-mTOR Pathway in Natural Killer Cell Effector Functions. Front. Immunol. *5*, 187.

Narni-Mancinelli, E., Chaix, J., Fenis, A., Kerdiles, Y.M., Yessaad, N., Reynders, A., Gregoire, C., Luche, H., Ugolini, S., Tomasello, E., et al. (2011). Fate mapping analysis of lymphoid cells expressing the NKp46 cell surface receptor. Proc. Natl. Acad. Sci. USA *108*, 18324–18329.

Nguyen, K.B., Cousens, L.P., Doughty, L.A., Pien, G.C., Durbin, J.E., and Biron, C.A. (2000). Interferon alpha/beta-mediated inhibition and promotion of interferon gamma: STAT1 resolves a paradox. Nat. Immunol. *1*, 70–76.

O'Sullivan, T.E., Johnson, L.R., Kang, H.H., and Sun, J.C. (2015). BNIP3- and BNIP3L-Mediated Mitophagy Promotes the Generation of Natural Killer Cell Memory. Immunity *43*, 331–342.

Patro, R., Duggal, G., Love, M.I., Irizarry, R.A., and Kingsford, C. (2017). Salmon provides fast and bias-aware quantification of transcript expression. Nat. Methods *14*, 417–419.

Rapp, M., Lau, C.M., Adams, N.M., Weizman, O.-E., O'Sullivan, T.E., Geary, C.D., and Sun, J.C. (2017). Core-binding factor β and Runx transcription factors promote adaptive natural killer cell responses. Sci. Immunol. *2*, eaan3796.

Rapp, M., Wiedemann, G.M., and Sun, J.C. (2018). Memory responses of innate lymphocytes and parallels with T cells. Semin. Immunopathol. *40*, 343–355.

Ring, A.M., Lin, J.-X., Feng, D., Mitra, S., Rickert, M., Bowman, G.R., Pande, V.S., Li, P., Moraga, I., Spolski, R., et al. (2012). Mechanistic and structural insight into the functional dichotomy between IL-2 and IL-15. Nat. Immunol. *13*, 1187–1195.

Schluns, K.S., Williams, K., Ma, A., Zheng, X.X., and Lefrançois, L. (2002). Cutting edge: requirement for IL-15 in the generation of primary and memory antigen-specific CD8 T cells. J. Immunol. *168*, 4827–4831.

Soneson, C., Love, M.I., and Robinson, M.D. (2015). Differential analyses for RNA-seq: transcript-level estimates improve gene-level inferences. F1000Res. *4*, 1521.

Speir, M.L., Zweig, A.S., Rosenbloom, K.R., Raney, B.J., Paten, B., Nejad, P., Lee, B.T., Learned, K., Karolchik, D., Hinrichs, A.S., et al. (2016). The UCSC Genome Browser database: 2016 update. Nucleic Acids Res. *44*, D717–D725.

Sugamura, K., Asao, H., Kondo, M., Tanaka, N., Ishii, N., Ohbo, K., Nakamura, M., and Takeshita, T. (1996). The interleukin-2 receptor gamma chain: its role in the multiple cytokine receptor complexes and T cell development in XSCID. Annu. Rev. Immunol. *14*, 179–205.

Sun, J.C., Beilke, J.N., and Lanier, L.L. (2009a). Adaptive immune features of natural killer cells. Nature *457*, 557–561.

Sun, J.C., Ma, A., and Lanier, L.L. (2009b). Cutting edge: IL-15-independent NK cell response to mouse cytomegalovirus infection. J. Immunol. *183*, 2911–2914.

Villarino, A.V., Sciumè, G., Davis, F.P., Iwata, S., Zitti, B., Robinson, G.W., Hennighausen, L., Kanno, Y., and O'Shea, J.J. (2017). Subset- and tissue-defined STAT5 thresholds control homeostasis and function of innate lymphoid cells. J. Exp. Med. *214*, 2999–3014.

Wu, C., Wang, X., Gadina, M., O'Shea, J.J., Presky, D.H., and Magram, J. (2000). IL-12 receptor beta 2 (IL-12R beta 2)-deficient mice are defective in IL-12-mediated signaling despite the presence of high affinity IL-12 binding sites. J. Immunol. *165*, 6221–6228.

Zhang, Y., Liu, T., Meyer, C.A., Eeckhoute, J., Johnson, D.S., Bernstein, B.E., Nusbaum, C., Myers, R.M., Brown, M., Li, W., and Liu, X.S. (2008). Model-based analysis of ChIP-Seq (MACS). Genome Biol. *9*, R137.

Zhu, L.J., Gazin, C., Lawson, N.D., Pagès, H., Lin, S.M., Lapointe, D.S., and Green, M.R. (2010). ChIPpeakAnno: a Bioconductor package to annotate ChIP-seq and ChIP-chip data. BMC Bioinformatics *11*, 237.

STAR★METHODS

KEY RESOURCES TABLE

REAGENT or RESOURCE	SOURCE	IDENTIFIER
Antibodies		
Anti-Mouse CD3ε (clone 17A2)	Tonbo Biosciences	Cat#25-0032; RRID: AB_2621619
Anti-Mouse TCRβ (clone H57-597)	BioLegend	Cat#109220; RRID: AB_893624
Anti-Mouse CD19 (clone 6D5)	BioLegend	Cat#115530; RRID: AB_830707
Anti-Mouse F4/80 (clone BM8.1)	BioLegend	Cat#123117; RRID: AB_893489
Anti-Mouse NK1.1 (clone PK136)	Tonbo Biosciences	Cat#65-5941; RRID: AB_2621910
Anti-Mouse NKp46 (clone 29A1.4)	BioLegend	Cat#137604; RRID: AB_2235755
Anti-Mouse Ly49H (clone 3D10)	eBioscience	Cat#11-5886-81; RRID: AB_1257160
Anti-Mouse CD45.1 (clone A20)	BioLegend	Cat#110729; RRID: AB_1134170
Anti-Mouse CD45.2 (clone 104)	BioLegend	Cat#109821; RRID: AB_493730
Anti-Mouse CD49b (clone Dx5)	BioLegend	Cat#108918; RRID: AB_2265144
Annexin V	BioLegend	Cat# 640943, RRID: AB_2616658
Anti-Mouse/Human CD11b (clone M1/70)	BioLegend	Cat#101223; RRID: AB_755985
Anti-CD27 (clone LG.7F9)	eBioscience	Cat#14-0271-81; RRID: AB_467182
Anti-Mouse KLRG1 (clone 2F1)	Tonbo Biosciences	Cat#50-5893; RRID: AB_2621800
Anti-Mouse Ly49D (clone 4E5)	BioLegend	Cat#138308; RRID: AB_10639939
Anti-Mouse Ly49A (clone YE1/48.10.6)	BioLegend	Cat#116810; RRID: AB_572013
Anti-Mouse Ly49C and Ly49I (clone 5E6)	BD Biosciences	Cat#553277; RRID: AB_394751
Anti-Mouse CD69 (clone H1.2F3)	BioLegend	Cat#104524; RRID: AB_2074979
Anti-Mouse Granzyme A (clone 3G8.5)	BioLegend	Cat#149704 RRID:AB_2565310
Anti-Human/Mouse Granzyme B (clone GB11)	BioLegend	Cat#515403; RRID: AB_2114575
Anti-Mouse IFN gamma (clone XMG1.2)	Tonbo Biosciences	Cat#20-7311; RRID: AB_2621616
Anti-Mouse CD107a (clone 1D4B)	BioLegend	Cat#121611; RRID: AB_1732051
Anti-Mouse Ki67 (Clone 16A8)	BioLegend	Cat# 652422; RRID: AB_2564490
InVivoMab Anti-Mouse CD8α (NK cell enrichment, clone 2.43)	Bio X Cell	Cat#BE0061; RRID: AB_1125541
InVivoMab Anti-Mouse CD4 (NK cell enrichment, clone GK1.5)	Bio X Cell	Cat#BE0003-1; RRID: AB_1107636
InVivoMab Anti-Mouse CD19 (NK cell enrichment, clone 1D3)	Bio X Cell	Cat#BE0150; RRID: AB_10949187
InVivoMab Anti-Mouse Ter-119 (NK cell enrichment, clone TER-119)	Bio X Cell	Cat#BE0183; RRID: AB_10949625
Human/Mouse STAT5a/b Pan Specific Antibody (ChIP, polyclonal)	R&D Systems	Cat#AF2168; RRID: AB_355174
Anti-STAT1 (M-22) (ChIP, polyclonal)	Santa Cruz Biotechnology	Cat#sc-592; RRID: AB_632434
Bacterial and Virus Strains		
Murine Cytomegalovirus (MCMV)	Johnson et al., 2016	Smith Strain
Chemicals, Peptides, and Recombinant Proteins		
Recombinant Mouse IL-12 Protein	R&D Sytems	Cat#419-ML
Recombinant Mouse IL-18	MBL	Cat#B002-5
Recombinant Mouse IL-2 Protein	R&D Systems	Cat#402-ML
Recombinant Mouse IL-15 Protein	R&D Systems	Cat#447-ML

(*Continued on next page*)

Continued

REAGENT or RESOURCE	SOURCE	IDENTIFIER
Recombinant Mouse IFNa 1 Protein	R&D Systems	Cat#12105-1
Phorbol 12-myristate 13-acetate (PMA)	Sigma-Aldrich	Cat#P8139
Ionomycin calcium salt from *Streptomyces conglobatus* (Ionomycin)	Sigma-Aldrich	Cat#I0634
Critical Commercial Assays		
QIAamp DNA Blood Mini Kit	QIAGEN	Cat#51106
TRIzol Reagent	Thermo Fisher Scientific	Cat#15596026
PicoPure RNA Isolation Kit	Thermo Fisher Scientific	Cat# KIT0204
Foxp3 Transcription Factor Staining Buffer Set	Thermo Fisher Scientific	Cat#00-5523-00
iQ SYBR Green Supermix	Bio-Rad	Cat#1708880
BioMag Goat Anti-Rat IgG (NK cell enrichment)	QIAGEN	Cat#310107
CellTrace Violet Cell Proliferation Kit	Thermo Fisher Scientific	Cat#C34557
Fixable Viability Dye eFluor 506	eBioscience	Cat#65-0866-18
FAM FLICA Poly Caspase Kit	Bio-Rad	Cat#ICT092
Deposited Data		
Raw Data Files for RNA and ChIP Sequencing	NCBI Gene	GSE106139
Raw Data Files for RNA and ChIP Sequencing	Expression Omnibus	GSE142821
Experimental Models: Organisms/Strains		
Mouse: WT or CD45.2: C57BL/6J	The Jackson Laboratory	Stock#000644; RRID:IMSR_JAX:000664
$Stat5^{fl/fl}$	Cui et al., 2004	N/A
$Il2rb^{fl/fl}$	The Jackson Laboratory	Stock#029657
$Il2ra^{fl/fl}$	Chinen et al., 2016	N/A
Mouse: $Nkp46^{iCre}$	Narni-Mancinelli et al., 2011	N/A
Mouse: $Ifnar1^{-/-}$: B6(Cg)-$Ifnar1^{tm1.2Ees}$/J	The Jackson Laboratory	Stock#028288; RRID: IMSR_JAX:028288
Mouse: $Stat1^{-/-}$	Meraz et al., 1996	N/A
Mouse: $Rag2^{-/-}$ $IL2rg^{-/-}$: C;129S4-$Rag2^{tm1.1Flv}$ $Il2rg^{tm1.1Flv}$/J	The Jackson Laboratory	Stock#014593; RRID:IMSR_JAX:014593
Mouse: $Il12rb2^{-/-}$	Wu et al., 2000	N/A
Mouse: $Stat4^{-/-}$	Kaplan et al., 1996	N/A
$Ubc^{Cre-ERT2}$; $Ndor1^{Tg(UBC-cre/ERT2)1Ejb}$	The Jackson Laboratory	Stock#007179
Mouse: $Klra8^{-/-}$ or Ly49H-deficient	Fodil-Cornu et al., 2008	N/A
Oligonucleotides		
Primers Forward MCMV IE-1: TCGCCCATCGTTTCGAGA	Johnson et al., 2016	N/A
Primer Reverse MCMV IE-1: TCTCGTAGGTCCACTGACGGA	Johnson et al., 2016	N/A
Software and Algorithms		
DESeq2 (v.1.14.1)	Love et al., 2014	http://bioconductor.org/packages/release/bioc/html/DESeq2.html
Trimmomatic (v.0.36)	Bolger et al., 2014	http://www.usadellab.org/cms/?page=trimmomatic
Bowtie2 (v.2.2.9)	Langmead and Salzberg, 2012	http://bowtie-bio.sourceforge.net/bowtie2/index.shtml
Salmon (v.0.10.2)	Patro et al., 2017	https://salmon.readthedocs.io/en/latest/salmon.html

(*Continued on next page*)

Continued

REAGENT or RESOURCE	SOURCE	IDENTIFIER
tximport (v.1.8.0)	Soneson et al., 2015	https://bioconductor.org/packages/release/bioc/html/tximport.html
R (v.3.3.3)	https://www.r-project.org/	https://www.r-project.org/
MACS2 (v.2.1.1.20160309)	Zhang et al., 2008	https://github.com/macs3-project/MACS
ChipPeakAnno (v.3.8.9)	Zhu et al., 2010	https://bioconductor.org/packages/release/bioc/html/ChIPpeakAnno.html
UCSC mm10 Known Gene Annotation Package(v.9)	Speir et al., 2016	https://bioconductor.org/packages/release/data/annotation/html/TxDb.Mmusculus.UCSC.mm10.knownGene.html
Irreproducible Discovery Rate (IDR) (v.2.0.3)	Li et al., 2011	https://www.encodeproject.org/software/idr/

RESOURCE AVAILABILITY

Lead contact

Further information and requests for resources and reagents should be directed to and will be fulfilled by the Lead Contact, Joseph Sun (sunj@mskcc.org).

Materials availability

This study did not generate new unique reagents.

Data and code availability

Data generated in this study have been deposited in the Gene Expression Omnibus. Accession numbers for RNA-seq and ChIP-seq are GSE142821and GSE140043, respectively.

EXPERIMENTAL MODEL AND SUBJECT DETAILS

Mice

All mice used in this study were housed and bred under specific pathogen-free conditions at Memorial Sloan Kettering Cancer Center (MSKCC) in accordance with all guidelines of the Institutional Animal Care and Use Committee (IACUC). The following strains were used, all on the C57BL/6 genetic background: C57BL/6 (CD45.2), B6.SJL (CD45.1), *NKp46*^{iCre} (Narni-Mancinelli et al., 2011), *Ubc*$^{ERT2\text{-}Cre}$, *NKp46*$^{Cre\text{-}ERT2}$, *Rosa26*$^{flox.tdTom}$, *Stat5*$^{fl/fl}$ (Cui et al., 2004), *Il2rb*$^{fl/fl}$ (JAX stock #029657; Chinen et al., 2016), *Il2ra*$^{fl/fl}$ (*CD25*$^{fl/fl}$) (Chinen et al., 2016), *Rag2*$^{-/-}$ *x Il2rg*$^{-/-}$ (Jackson), *Rag2*$^{-/-}$ *x Klra8*$^{-/-}$ (*Ly49h*$^{-/-}$), and *Klra8*$^{-/-}$ (*Ly49h*$^{-/-}$) (Fodil-Cornu et al., 2008). Experiments were conducted using age- and gender-matched mice in accordance with approved institutional protocols. Animals were typically 6-10 weeks old at the time of use and consisted of males and females.

Mixed bone marrow chimeric mice were generated by lethally irradiating (900 cGy) host CD45.1xCD45.2 mice, which were then reconstituted with a 1:1 or 5:1 (for *NK*^{Cre} *x Stat5*$^{fl/+}$ donors, which possess lower numbers of NK cells) KO:WT mixture of bone marrow cells from WT (CD45.1) and knockout (CD45.2) donor mice. Hosts were co-injected with anti-NK1.1 (clone PK136) to deplete residual mature NK cells.

METHOD DETAILS

Virus infection

MCMV (Smith strain) was serially passaged through BALB/c hosts twice, then viral stocks were prepared by dissociating salivary glands 3 weeks after infection with a dounce homogenizer. Intraperitoneal infections with MCMV were performed as previously described (Rapp et al., 2017).

Adoptive transfer studies

Adoptive transfer experiments were performed by mixing splenocytes from WT (CD45.1) and knockout (CD45.2) mice (or from mixed bone marrow chimeric mice) to achieve equal numbers of Ly49H^{+}KLRG1^{lo} NK cells, and injecting i.v. into adult *Klra8*$^{-/-}$ or *Rag2*$^{-/-}$ *x Il2rg*$^{-/-}$ mice. Recipient mice were then infected by i.p. injection of 7.5×10^2 PFU of MCMV. Experimental mixed bone marrow chimera mice were infected by i.p. injection of 7.5×10^3 PFU of MCMV. For survival studies, mice were infected by i.p. injection of 4×10^4 PFU of MCMV (Johnson et al., 2016).

Tamoxifen and antibody treatment

Mice were administered 4 mg tamoxifen dissolved in 200 μL corn oil by oral gavage. Control mice received 200 μL corn oil. Anti-IL-2 treatment was administered every second day with 300 μg anti-IL-2 (150 μg each of clone JES6-1A12 and S4B6-1, BioXCell). Anti-IL15 treatment was performed daily with 25 μg anti-IL-15 antibody (clone AIO.3, BioXCell).

Flow cytometry and cell sorting

Single cell suspensions were prepared and stained with indicated surface or intracellular antibodies (BD Biosciences, eBioscience, BioLegend, Tonbo, and R&D Systems), as previously described (Adams et al., 2019). Apoptosis was evaluated by caspase activity staining using the FLICA poly caspase assay kit (Immunochemistry Technologies). NK cell proliferation was analyzed by labeling cells with 5 μM Cell Trace Violet (CTV, Invitrogen) prior to transfer and infection. Flow cytometry was performed on an LSR II (BD). Cell sorting was performed on an Aria II cytometer (BD). All data were analyzed with FlowJo software (TreeStar). Flow cytometry of purified lymphocytes was performed using the following fluorophore-conjugated antibodies: CD3ε (17A2), TCRβ (H57-597), CD19 (ID3), F4/80 (BM8.1), NK1.1 (PK136), Ly49H (3D10), CD45.1 (A20), CD45.2 (104), CD11b (M1/70), CD27 (LG.3A10), KLRG1 (2F1), Ly49D (4E5), Ly49A (YE1/48.10.6), Ly49C/I (5E6), CD69 (H1.2F3), Granzyme A (3G8.5), Granzyme B (GB11), IFN-γ (XMG1.2), CD107a (1D4B), and CD49b (DX5).

ChIP-seq and analysis

Chromatin immunoprecipitation sequencing (ChIP-seq) for STAT4 and H3K4me3 were performed and described previously by our lab (Lau et al., 2018; Rapp et al., 2017). For the STAT5 ChIP, 4-5 × 10^6 NK cells ($CD3\varepsilon^-$ $TCRb^-$ $CD19^-$ $F4/80^-$ $NK1.1^+$) were stimulated with or without 20 ng/mL recombinant mouse IL-2 (Fisher Scientific) plus 20 ng/ml recombinant mouse IL-15 (R&D Systems). DNA and proteins were cross-linked for 8 min at room temperature using 1% formaldehyde. Cross-linked cells incubated in cell lysis buffer (25 mM HEPES, 1.5 mM $MgCl_2$, 10mM KCl, 0.1% NP-40, 1mM DTT, 1x proteinase inhibitor) and nuclei were isolated by centrifugation at 5400 rpm for 5.5 min. Chromatin was sheared using a Covaris ultrasonicator. ChIP was performed using 8 μg anti-Stat5 (#AF2168, R&D Systems) and Dynabeads Protein G (Invitrogen). Immunoprecipitated DNA was quantified by PicoGreen and the size was evaluated by Agilent BioAnalyzer. Whenever possible, fragments between 100 and 600 bp were size selected using aMPure XP beads (Beckman Coulter catalog # A63882) and Illumina libraries were prepared using the KAPA HTP Library Preparation Kit (Kapa Biosystems KK8234) according to the manufacturer's instructions with up to 10ng input DNA and 8-11 cycles of PCR. Barcoded libraries were run on a HiSeq 4000 in a 50bp/50bp paired end run, using the HiSeq 3000/4000 SBS Kit (Illumina).

STAT5 ChIP-seq reads generated in this study and those generated elsewhere (GSE100674; Villarino et al., 2017) were trimmed to remove low quality reads using Trimmomatic (v.0.36) (Bolger et al., 2014). Trimmed reads were mapped to the *Mus musculus* genome (mm10 assembly) using Bowtie2 (v2.2.9) (Langmead and Salzberg, 2012), and MACS2 (v.2.1.1.20160309) (Zhang et al., 2008) was used with arguments "-f BAM -p 0.05 -m 2 50" for single-end peak calling. For each condition, irreproducible discovery rate (IDR) calculations using scripts provided by the ENCODE project (https://www.encodeproject.org/software/idr/; v2.0.3) (Li et al., 2011) were performed on all pairs of replicates using an oracle peak list derived from all samples within that condition, keeping reproducible peaks showing an IDR value of 0.05 or less in all pairs. A union of IDR-thresholded peaks generated from both unstimulated and stimulated conditions comprised the final peak list 1,201 peaks, annotated with ChipPeakAnno (v.3.8.9) (Zhu et al., 2010) using the UCSC Known Gene model (Speir et al., 2016).

RNA-seq and analysis

RNA-seq processing and analyses for MCMV time course and STAT4-deficient Ly49H+ NK cells were performed and described previously (Lau et al., 2018). RNA-seq processing and analyses from IL12R-deficient NK cells was performed in the same manner as STAT4-deficient NK cells described above. RNA was isolated from sorted CD45.1+ or CD45.2+ NK cells (TCRb- CD3- NK1.1+ Ly49H+) from WT versus NK^{Cre} x $Stat5^{fl/+}$ splenocytes using the PicoPure RNA Isolation Kit (Thermo Fisher). After RiboGreen quantification and quality control by Agilent BioAnalyzer, 0.705-2ng total RNA with RNA integrity numbers ranging from 6.5 to 10 underwent amplification using the SMART-Seq v4 Ultra Low Input RNA Kit (Clontech catalog # 63488), with 12 cycles of amplification. Subsequently, 10ng of amplified cDNA was used to prepare libraries with the KAPA Hyper Prep Kit (Kapa Biosystems KK8504) using 8 cycles of PCR. Samples were barcoded and run on a HiSeq 4000 in a 50bp/50bp paired end run, using the HiSeq 3000/4000 SBS Kit (Illumina).

RNA-seq sample reads were trimmed as above. Transcript quantification was based on the mm10 UCSC Known Gene model and performed using the quasi-mapping-based mode of Salmon (v.0.10.2) (Patro et al., 2017) correcting for potential GC bias. Transcripts were summarized to gene level using tximport (v.1.8.0) (Soneson et al., 2015). Differential analyses were executed with DESeq2 (v1.14.1) (Love et al., 2014). Normalized counts are raw counts scaled by per-sample size factors calculated by DESeq2.

QUANTIFICATION AND STATISTICAL ANALYSIS

Statistical analyses

Data are shown as mean ± SEM in all graphs and statistical differences were calculated using a two-tailed unpaired Student's t test, unless otherwise indicated. p values < 0.05 were considered significant. All statistical analyses and plots were produced in GraphPad Prism or R (v3.3.3).

Cell Reports, Volume *33*

Supplemental Information

Divergent Role for STAT5 in the Adaptive Responses of Natural Killer Cells

Gabriela M. Wiedemann, Simon Grassmann, Colleen M. Lau, Moritz Rapp, Alejandro V. Villarino, Christin Friedrich, Georg Gasteiger, John J. O'Shea, and Joseph C. Sun

Supplementary Material

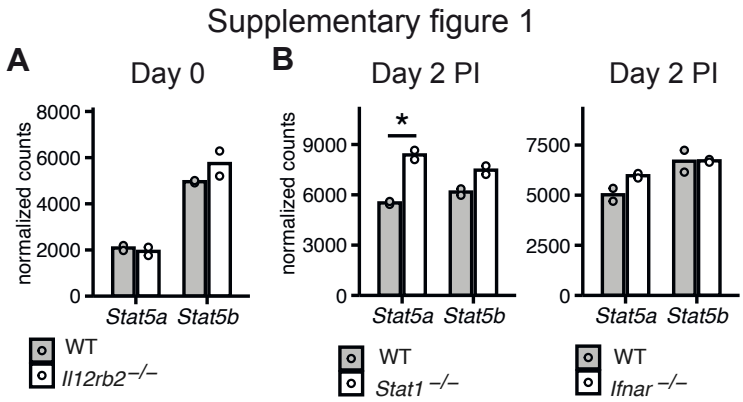

Fig. S1. IL-12- and STAT4-dependent induction of STAT5 in NK cells during MCMV infection. Related to Figure 1.
(**A**) RNA-seq on WT vs. *Il12rb2*$^{-/-}$ NK cells from mixed BMC on day 0 (uninfected). Normalized counts of *Stat5a* and *Stat5b* are displayed. (**B**) RNA-seq on WT vs. *Stat1*$^{-/-}$ or *Ifnar*$^{-/-}$ from mixed BMC on day 2 PI. Normalized counts of *Stat5a* and *Stat5b* are displayed.

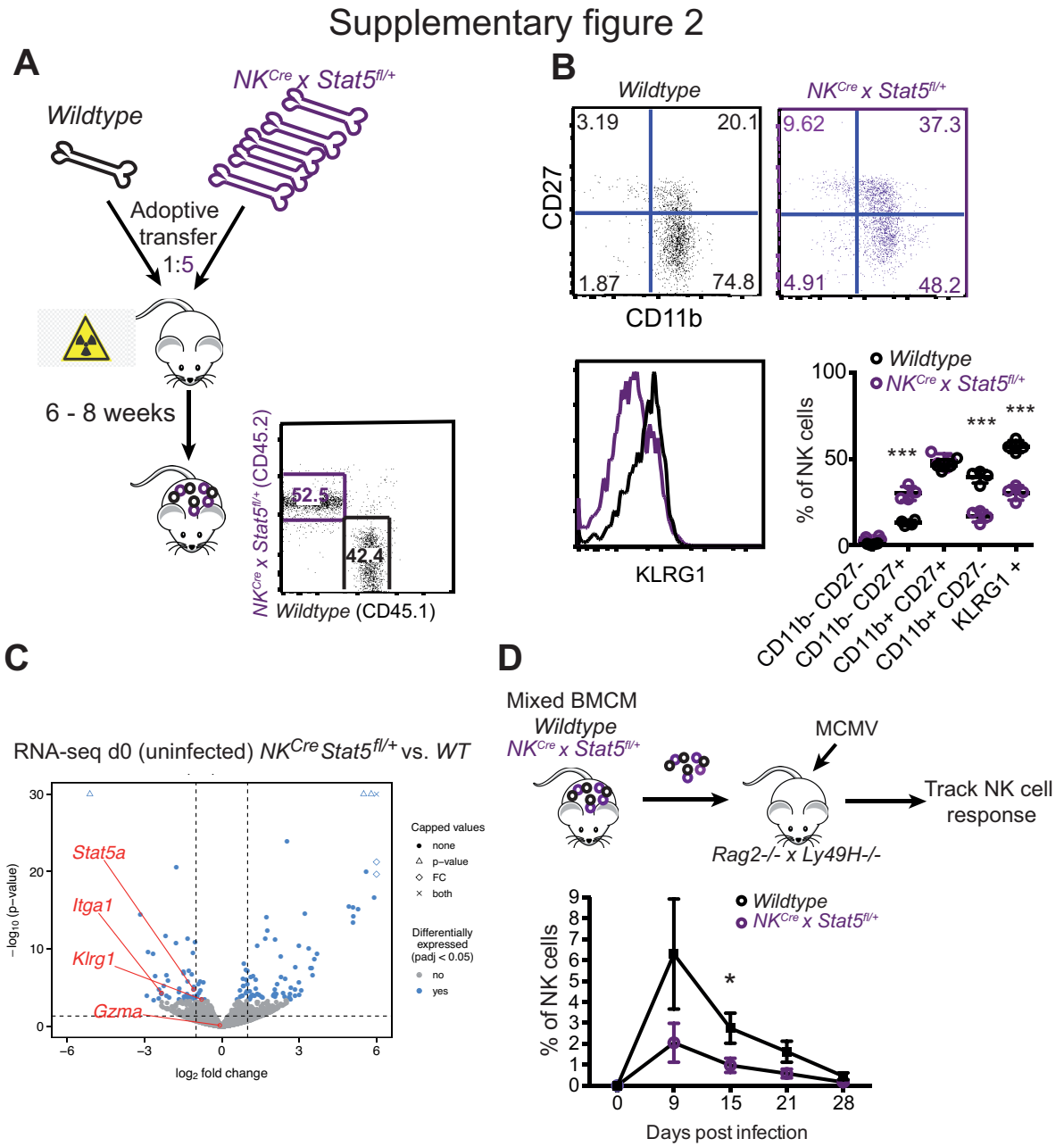

Fig. S2. STAT5-dependent anti-viral NK cell response. Related to figure 2.
(**A-C**). Mixed bone marrow chimeras (mBMC) were generated by lethal irradiation (900 cGy) of host mice, which were then reconstituted with a 1:5 mixture of bone marrow cells from WT and *NK^{Cre} x Stat5$^{fl/+}$* donor mice. (**A**) Experimental schematic of mBMC generation. Representative flow blot of NK cell reconstitution 8 weeks after reconstitution. (**B**) Analysis of NK cell maturation markers on WT and *NK^{Cre} x Stat5$^{fl/+}$* NK cells in mBMC 8 weeks post reconstitution. (Data is representative of at least 3 experiments). (**C**) Volcano blot of RNA-seq data on uninfected (d0) Ly49H^{+} WT or *NK^{Cre} x Stat5$^{fl/+}$* NK cells from mBMC. Blue dots show differentially expressed (FDR < 0.05) genes. Horizontal line indicates p = 0.05, and vertical lines show absolute log2 fold change = 1. (**D**) Splenocytes from mixed WT : *NK^{Cre} x Stat5$^{fl/+}$* BMC where adoptively transferred into *Rag2$^{-/-}$ x Ly49h$^{-/-}$* mice and infected with MCMV. Graph shows percentage of Ly49H+ WT or KO NK cells of total NK cells over the course of infection. Data is representative of 2 independent experiments (n=3-4). All error bars indicate SEM.

Supplementary figure 3

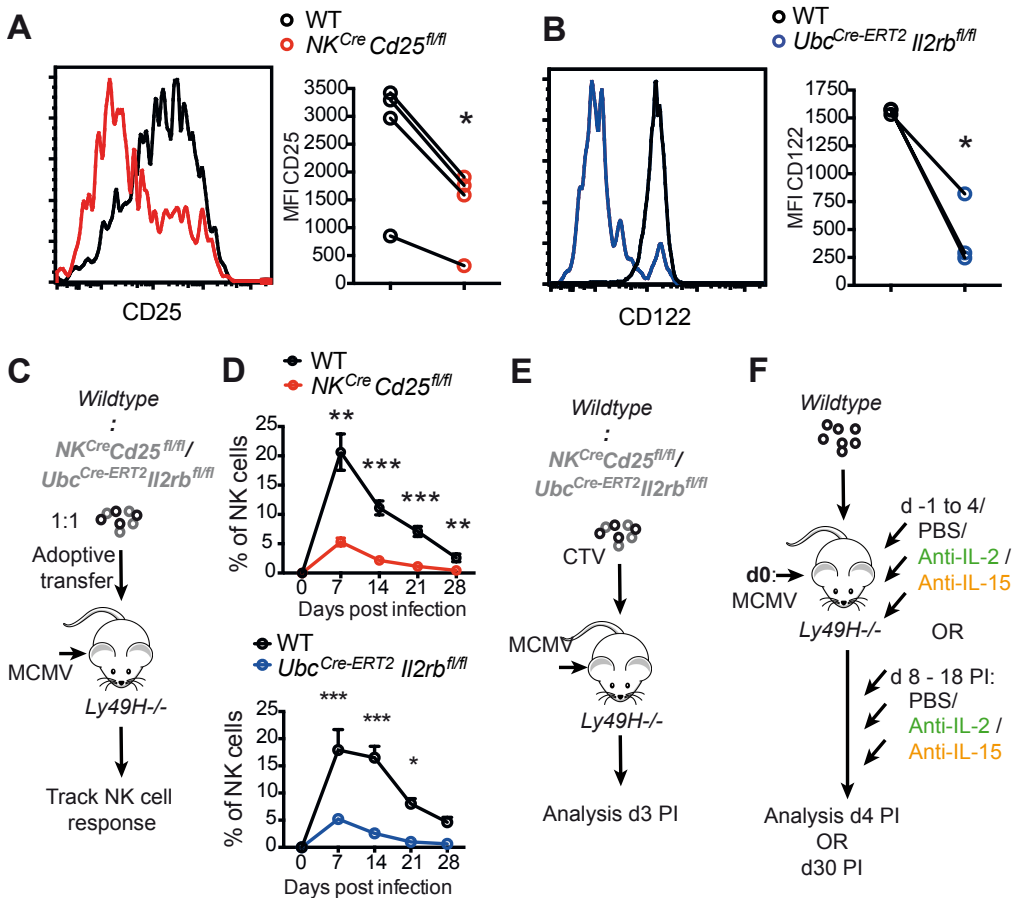

Fig. S3. Both IL-2 and IL-15 drive NK cell expansion *in vivo*. Related to figures 3 and 4. (**A-C**) Equal numbers of WT and *Ubc*$^{Cre\text{-}ERT2}$ *x Il2rb*$^{fl/fl}$ or *NK*^{Cre} *x CD25*$^{fl/fl}$ NK cells were transferred into *Ly49h*$^{-/-}$ mice. Mice transferred with *Ubc*$^{Cre\text{-}ERT2}$ *x Il2rb*$^{fl/fl}$ NK cells were treated with tamoxifen on days -3, -2 and -1 before infection with MCMV. Following MCMV infection, relative percentages of Ly49H^{+} WT and KO NK cells are displayed (n = 4-5). (**A**) Analysis of CD25 expression on WT and *NK*^{Cre} *x CD25*$^{fl/fl}$ NK cells on day 3 PI. Data is representative of 2 independent experiments. (**B**) Analysis of CD122 expression on WT *Ubc*$^{Cre\text{-}ERT1}$ *x Il2rb*$^{fl/fl}$ on day 3 PI. Data is representative of 2 independent experiments. (**C**) Experimental schematic of adoptive transfer and infection. (**D**) Graphs display percentage of Ly49H+ WT and *NK*^{Cre} *x CD25*$^{fl/fl}$ or *Ubc*$^{Cre\text{-}ERT2}$ *x Il2rb*$^{fl/fl}$ NK cells of total NK cells over the course of infection. Data is representative of at least 2 independent experiments (n=4-5). (**E**). Experimental schematic of CTV labeling and analysis: NK cells from WT mice, *NK*^{Cre} *x CD25*$^{fl/fl}$ mice, or *Ubc*$^{Cre\text{-}ERT2}$ *x Il2rb*$^{fl/fl}$ mice treated with tamoxifen on days -3, -2 and -1 were labeled with CTV and transferred into *Ly49h*$^{-/-}$ mice, followed by infection with MCMV. (**F**) Experimental schematic of antibody-mediated IL-2 and IL-15 depletion: WT Ly49H^{+} NK cells were transferred into *Ly49h*$^{-/-}$ mice treated with PBS, anti-IL-2, or anti-IL-15 on day -1 to 4 PI (early) or days 8 to 18 PI (late) and analyzed on day 4 PI (early) or day 30 PI (late). All error bars indicate SEM.